GLIMPSE Quality Assurance v1.0

Ed Churchwell, Brian Babler, Steve Bracker, Martin Cohen, Remy Indebetouw,
Marilyn Meade, Christer Watson, Barbara Whitney
Jan. 24, 2006

Contents

Preface

This version of the GLIMPSE Quality Assurance document examines all aspects of the survey that affects the quality of the GLIMPSE Point Source Catalog, Archive, and mosaicked images. The final release of these source lists in 2006 may have different selection criteria and flux limits, based on our continuing analysis of the data. Any such modifications to the Catalog and/or Archive will be carefully described in subsequent versions of this document.

I. Introduction

In this document we describe the quality of the Galactic Legacy Mid-Plane Survey Extraordinaire (GLIMPSE) data products. This will include a brief description of the observing strategy, source selection criteria, the reliability and completeness of the point source catalog and archive, photometric accuracy, astrometric accuracy, correction for instrumental artifacts and cosmic ray hits, and the relevant detection, saturation, and confusion limits over which the data products are valid. Determination of these parameters relied heavily on the observation strategy validation (OSV) data taken before the program proper began and made use of simulated IRAC data with known stellar fluxes.

The GLIMPSE program produces two lists of extracted point sources; a high reliability point source catalog (henceforth referred to as the Catalog) and an Archive consisting of extracted point sources down to noise levels of approximately 5σ. The criteria for inclusion in both of these lists are discussed in §IV.

The GLIMPSE Catalog and Archive have quality flags that indicate possible problems encountered in extracting the position and flux density of a source such as banding and being near a bright star. The type of flag conveys the nature of the problem. The flags are described in the GLIMPSE Data Products Description[1]. The total number of sources in version 1 of the Catalog and Archive are 30,252,689 and 47,722,247, respectively.

II. GLIMPSE Observing Strategy

The GLIMPSE project observed the Galactic plane ($10^0 \leq |\ell| \leq 65^0$ and $|\ell| \leq 1^0$)[2] in the four IRAC bands in 400 hours. The observations were completed in 8 campaigns of about 50 hours each. Each campaign observed about 15 degrees of longitude ($|b| \leq 1^0$) or about 30 square degrees with adequate overlap between campaigns to insure that no areas were missed. Campaigns were separated by weeks to months, depending on visibility requirements. Each campaign was observed by tiling the area with long astronomical observing requests (AORs; see the Spitzer Observer's Manual). The AORs were rectangles, about 4 frames wide (fully spaced except for an overlap of 8-20 pixels) and about 100 frames long (spaced in half-frame increments). Thus, each position on the sky was observed at least twice per band. These long AORs typically make an angle with the line of constant galactic latitude of about 30 degrees. To minimize the change in this angle during a single campaign, AORs were observed in quick succession.

III. The Observation Strategy Validation Data

The OSV data consisted of ten independent observations of a 0.8^0 x 2^0 region centered at G283.4-0.3 using the same observing technique that we used for the GLIMPSE survey. The surveyed region contained the bright, massive star formation region RCW49, as well as areas with almost no diffuse dust emission so the whole range of diffuse brightness and stellar density expected in the GLIMPSE survey was included in the OSV region. Observations were taken in array coordinates using half-frame steps along the column axis over the full range of galactic latitude. Full-frame offsets, except for overlaps of 8-20 pixels, were used perpendicular to the array column axis. This technique provided at least two observations of every point in the survey. The survey was repeated five times with five

[1] www.astro.wisc.edu/glimpse/docs.html

[2] $|\ell|$ implies the angular distance from the Galactic center.

different frame edge overlaps of 8, 10, 12, 15, and 20 pixels giving a minimum of ten independent observations of every direction in the OSV survey area. It was established that an overlap of 12-15 pixels was required to insure complete coverage. Each observation both for the OSV and GLIMPSE surveys had a "frame time" of 2s resulting in an effective exposure time of 1.2s. The time between exposures was 20s, which provided time for readout and telescope repositioning. The OSV data were used to determine the selection criteria for inclusion in the GLIMPSE Catalog, photometric and astrometric accuracies, and empirically determine detection and saturation limits.

IV. Point Source Selection Criteria

Establishment of point source selection criteria for the GLIMPSE Catalog was a multi-step process. Because the GLIMPSE Catalog was required to have a reliability ≥99.5% (i.e. ≤5 false sources out of a thousand), we had to determine selection criteria that insured that this standard was met with only two observations. To do this, we first simulated ten sets of truth images of the same field (images with stars of known positions and magnitudes; our external truth table) that could be used to establish criteria to form an internal truth table (i.e. objects that could be identified as true stars without prior knowledge of what is real and what is false) in the OSV field. The simulated truth images were processed ten times by the GLIMPSE pipeline and the extracted sources were checked against the external truth table to determine the minimum number of times that a source had to be independently detected in a given IRAC band to constitute a true source. This was established by comparing the extracted source with the external truth table. Brightness thresholds were also set in this process. Having established the number of times a source had to be detected to constitute a true source from the simulated truth images (i.e. the rules for establishing an internal truth table), we could then use our OSV images, which had been observed ten times in all four IRAC bands, to establish an internal truth table for those data. Having an internal truth table for the OSV region then permitted us to empirically determine the minimum selection criteria for inclusion of sources into the Catalog when only two observations are available, as in the GLIMPSE survey, and that satisfy the reliability requirement.

Simulated Truth Images

Truth images were simulated from MSX (Midcourse Space Experiment, Price et al. 2001), 2MASS (Two Micron All Sky Survey, Cutrie et al. 2003[3]), and IRSky (Wainscoat et al. 1992; Cohen 1993, 1994). MSX point sources were removed from the MSX images to produce a diffuse background which was scaled for the different IRAC bands. The method was tuned to produce a background free of stellar residuals, not to most accurately preserve the flux of sources in the catalog. The 2MASS point source catalog was augmented at the faint and bright ends to match the IRSky stellar luminosity function and inserted into the synthesized images with the appropriate IRAC point spread function using Matt Ashby's IRAC Science Data Simulator[4] (ISDS). Augmentation of the bright sources was necessary because the 2MASS source list (2nd Release) was missing a lot of the brightest stars that produced large diffraction spikes in the 2MASS data. At the faint end, we wanted to have known stars well below our expected confusion limit to fully test our source extraction

[3] http://www.ipac.caltech.edu/2mass/release/allsky/doc/explsup.html
[4] http://cfa-www.harvard.edu/~mashby/isds.html

routines at the faint end and to properly include the background introduced by unresolved faint stars. The inclusion of these undetectable faint stars as well as diffuse MSX background (which also contains unresolved faint objects) means that the diffuse background in the simulated data is probably a slight over-estimate, thereby providing a conservative analysis of our photometric routines. The simulated images were "flat-fielded" using the same gain maps that were originally used by ISDS, resulting in images that were photometrically calibrated but have higher noise at the frame edges because of vignetting and decreased sensitivity there. The simulated images, each with added noise and instrumental artifacts, were processed through the GLIMPSE pipeline and the extracted point sources were compared with the external truth table. It was found that 7 5σ detections out of 10 observations in any band or an adjacent band (the "7 or 7" criterion) of the same synthetic field provided a highly reliable internal truth table.

OSV Data: Establishment of an Internal Truth Table and Source Selection Criteria

Having established a robust criterion for producing an internal truth table for a field in which no external truth table exists (such as the OSV data), we processed the ten independent OSV observations through the GLIMPSE pipeline to establish an internal truth table for this region. The internal truth table permitted us to determine the reliability of stars extracted by our pipeline from the OSV data. We then proceeded to process the OSV data precisely in the same way the GLIMPSE survey data were processed (i.e. half-frame overlapping pairs with each frame being processed separately). This was repeated five times (ten observations taken two at a time) for each set of selection criteria that were tried. After many iterations it was found that the minimum criteria for including a star in the Catalog with a reliability ≥99.5% when only two observations are available (as is the case for the GLIMPSE survey) are: flux densities >0.6, >0.4, >2.0, and >10 mJy in bands 1, 2, 3, and 4, respectively, and two ≥5σ detections in one band and at least one detection at >3σ of the same source in an adjacent band (the "2+1" criterion). Generally, the flux density limits insure that the detections are >5σ, but in the brightest background regions this may be violated. In addition, sources are excluded from the Catalog that lie in the wings of saturated sources (see Table 2) and bright sources in the nonlinear range of the detectors, sources in areas that exceed the confusion limit (see §VIII), sources falling on hot or dead pixels within 3 pixels of source center, and sources lying within 3 pixels of the edge of a frame. The 2+1 criterion also excludes cosmic rays from the catalog.

Selection criteria for the GLIMPSE Point Source Archive (hereafter the "Archive") are less stringent than those for the Catalog. If a source is detected with S/N≥5 twice in either the same band or once in two different bands, it is included in the Archive. In both the Catalog and Archive, if a source was detected in one or more of the other bands (the bands not used for the selection criteria), those magnitudes are also listed if they have S/N≥3..

The OSV data were also used to test our observing strategy. For example, OSV data indicated 12 pixel overlap was large enough to insure full coverage from one AOR to the next and that overlaps between IRAC campaigns were adequate. Subsequent observations showed that 15 pixel overlap was required in some areas, consequently most of the survey has 15 pixel overlap. The OSV data brought to our attention that spatially variable background emission, especially in band 4, tends to obfuscate point source extraction.

V. Reliability and Completeness

Reliability is defined as the ratio of true sources found divided by the total number of sources (true plus false) and completeness is the number of true sources found divided by the total number of true sources. In §IV, we described how internal truth tables were established for the OSV region and how they were used to determine selection criteria that satisfy the high reliability requirements. In this section we show the dependence of reliability on flux density resulting from these analyses for all IRAC bands.

The reliability plots shown in Figure 1 include the entire OSV region and contain all sources that satisfy the selection criteria listed in §IV. The total number of point sources in the analysis shown in Fig. 1 were: 41,140 (band 1), 37,660 (band 2), 11,475 (band 3), and 2004 (band 4). From Fig. 1 we see that reliability ≥99.5% is achieved at >0.6 mJy (<14.2 mag), >0.4 mJy (<14.1 mag), >2 mJy (<11.9 mag), and >10 mJy (<9.5 mag) in IRAC bands 1, 2,

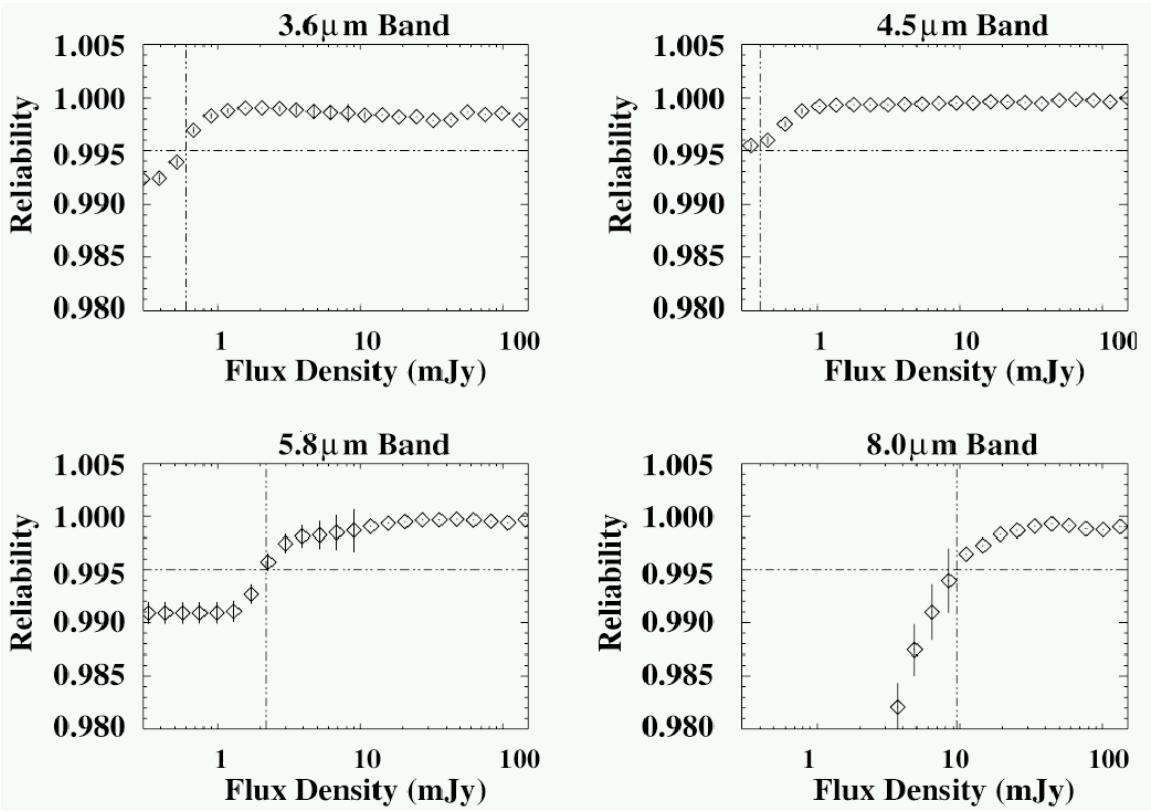

Figure 1. Reliability versus flux density for each of the IRAC bands. Reliability was determined as described in the text. A reliability >99.5% is reached at the minimum flux density indicated by the vertical dashed line.

3, and 4, respectively[5]. Generally, these flux density limits insure that a source is detected with a S/N well in excess of 5 except for a very small fraction of sources located in the brightest background regions. The (2+1) selection criterion for the Catalog is a more stringent criterion than the (7or7) criterion used for the internal truth table. This is illustrated

[5] See the "GLIMPSE Legacy Science Data Products" document for the zero points for conversion from flux density to magnitudes at http://www.astro.wisc.edu/glimpse/docs.html

by the fact that the (2+1) criterion only selects about 66 to 67% of the sources in the truth tables using the (7or7) criterion.

Since undetected true sources are not included in the internal truth table, completeness cannot be accurately assessed by comparison with an internal truth table and no external truth table exists for the OSV region. To assess the completeness of the Catalog and Archive we must either compare with a reliable model that predicts the number of sources in a given area of the Galaxy or with an observed catalog that has similar spatial resolution, sensitivity, and wavelength coverage. IRAS, MSX, and COBE/DIRBE do not have the combination of sensitivity, spatial resolution, and wavelength coverage that Spitzer/IRAC has. 2MASS and IRAC have about the same resolution and sensitivity but not the same wavelength coverage. ISO/ISOCAM does not cover a large enough contiguous area to provide reliable statistics and its band passes are not the same as those of IRAC.

Fig. 2 shows a comparison of the Catalog and Archive source counts in IRAC band 2 with predictions of the latest version of the IRSky model for the Galaxy modified for the IRAC bands and includes the warp of the disk (Cohen 2006) in the direction of $l=311^0$. Although not necessarily a reliable test of completeness, this comparison shows that the Catalog and Archive are in good agreement with the SKY model and at least as complete. Probably the best indicator of completeness of the Catalog is the fact that only about 66% of the sources in the internal truth table for the OSV region actually made it into the Catalog. Completeness is low because we have put most emphasis on high reliability for the Catalog. The Archive, of course will be more complete but less reliable because the selection criteria are less stringent than for the Catalog. The number of sources in the Catalog are only ~0.63 that in the Archive (difficult to see on the log scale in Fig. 2) in the magnitude range where the detectors are not near saturation or the detection limit.

Completeness also depends on source density and brightness as illustrated in Figure 7 (see §VIII), which shows that even at densities of 200 sources per square arcmin completeness is greater than 95% for sources brighter than 12^{th} magnitude, but only about 78% for sources brighter than 14^{th} magnitude. The mean density of sources over the whole survey in the Catalog and Archive is only 38 sq arcmin^{-2} and 59 sq arcmin^{-2}, respectively.

VI. Photometric Accuracy

To produce color-magnitude and color-color diagrams of sufficient accuracy for quantitative analyses, our goal was to achieve point source photometric accuracy ≤0.2 mag. A summary of the fraction of sources in both the Archive and Catalog that achieve this level of accuracy is given in Table 1 broken down by IRAC band. Every source in the Archive and Catalog have magnitude error bars that indicate if they exceed the 0.2 mag goal along with other flags that indicate a host of other possible effects that might affect the measured properties of the object.

The large percentage of sources that exceed the target photometric accuracy is a result of the selection rules for inclusion in the Catalog and Archive. We include a source that satisfies the selection rules in any one or two adjacent IRAC bands even if they do not satisfy the selection rules in the other bands. Having established that an object is a true source, we include its flux density in all bands where it has been clearly detected at ≥3σ even if it does not meet the ≥5σ criterion in those bands. Because magnitudes are reported for true sources in bands that do not satisfy the selection rules, these sources often have S/N<5 and photometric errors greater than 0.2 mag. In fact, errors of 0.2 mag correspond to S/N=5.43.

Thus, the number of sources that exceed the 0.2 mag error is a measure of the number of sources that have S/N<5.43 in bands where the selection criteria are not satisfied. Bands 3 and 4,

Table 1: Photometric Accuracy of the GLIMPSE Sources

	Band 1	**Band 2**	**Band 3**	**Band 4**
Catalog				
No. with error >0.2mag	622,096	3,476,464	3,773,154	2,031,098
Total no. of entries	29,974,376	29,965,902	11,473,693	8,791,651
% with errors >0.2mag	2.08%	11.60%	32.89%	23.10%
Archive				
No. with error >0.2mag	2,983,624	9,567,669	4,312,678	2,546,927
Total no. of entries	46,631,407	41,284,808	12,384,090	9,748,115
% with errors >0.2mag	6.40%	23.17%	34.82%	26.13%

which have the lowest sensitivity of the four IRAC bands, have the largest percent of sources with errors >0.2mag. Since the source list was truncated at S/N>3, no sources should be included with photometric errors >0.36 mag.

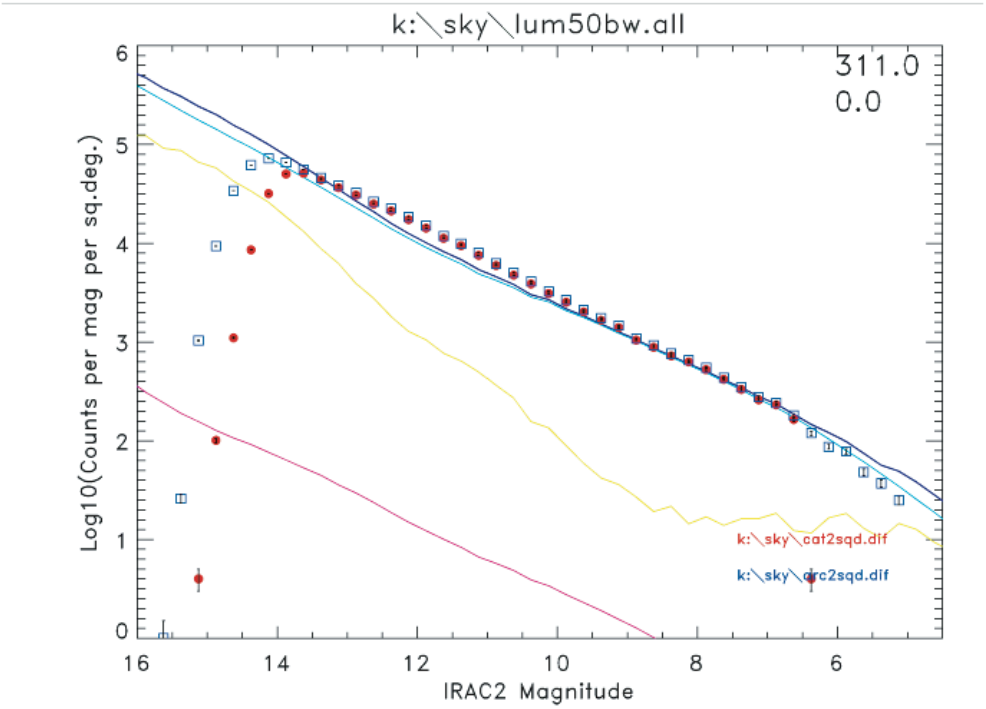

Figure 2. Comparison of the Catalog and Archive differential source counts with the SKY model of Cohen 1993, 1994) for the Galaxy toward longitude l=311^0, b=0^0 . The red dots are from the Catalog and the blue squares are from the Archive. The red, yellow, blue and purple curves are components of the SKY model and the black curve is the total number of sources (sum of the components). The sensitivity limits occur near 14th mag.

The GLIMPSE survey used a network of calibration stars distributed throughout the survey area to track the SSC calibration and to check the accuracy of GLIMPSE extracted flux densities. We had 277 possible calibrator sources distributed throughout the survey area but some were saturated and not used. We actually used 123 calibrators in Band 1, 138 in Band 2, 242 in Band 3, and 240 in Band 4.

In Figure 3, we plot the predicted flux densities of these calibration sources against the GLIMPSE extracted flux densities for each IRAC band. The predicted flux densities are from Cohen (2006). The two solid lines that flare out from the origin about the 45 degree line represent photometric errors of 0.2 mag. The vertical dashed lines are our best estimate of the saturation limits of the IRAC detectors. The figure shows that at flux densities lower than the saturation limits, the GLIMPSE extracted flux densities are well within the 0.2mag errors; this is true even somewhat above the saturation limits. The calibration sources, however, represent a very small fraction of the sources in the Catalog and Archive. Only one of the non-saturated calibrators exceeded the 0.2mag limit (see Fig. 3 band 4).

VII. Astrometric Accuracy

GLIMPSE positional accuracy is limited by the: astrometry of the sources used to define the reference frame (2MASS); accuracy of matching to that reference frame; precision of GLIMPSE point source extraction; and, accumulation of errors during bandmerging.

2MASS has been found to have <100mas astrometric accuracy for sources of intermediate brightness[6] (Ks ~5 to ~14 mag). Brighter sources in the 2MASS Catalog are derived at least in part from other datasets, and the astrometric accuracy degrades to ~150mas. Typically, ~25 sources are matched between each IRAC frame and the 2MASS Catalog by the SSC pipeline, therefore the IRAC pointing correction can be no better than about $150\text{mas}/25^{1/2}$ = 30mas. In practice, this process is limited by the precision of PSF-fitting using SSC's APEX source extractor (IRAC is under-sampled at the shorter wavelength bands), and by the definition of the centroid of the IRAC PSF. The quoted error of the position refinement process is <200 mas (Spitzer Observer's Manual, Chap 6, section 6.3.2.4).

GLIMPSE uses DAOPHOT-based PSF fitting (Stetson 1987) to extract point sources, which is also subject to astrometric errors due to under-sampling of that PSF. We expect the precision for any individual source extraction to be about 0.1 pixel, or 120mas. Combination with the 150mas accuracy of the frame results in 200mas accuracy of a single detection. Sources detected in multiple bands will have the weighted mean position reported, and as long as the cross-identification is correct, the positional accuracy could improve to $200/8^{1/2}$ = 70mas for sources detected twice in each of four bands.

Differences between GLIMPSE and 2MASS positions in RA and Dec (also in ℓ and b) show both systematic offsets of ~100 mas and random dispersions of ~100mas. This is shown in Figure 4 where we show the distribution of measured position differences sampled every 10 degrees in longitude in the southern Galactic plane. Similar results are found for the northern plane. We also measured position differences sampled over 12 arcmin intervals and find similar values for systematic and random position differences.

[6] http://spider.ipac.caltech.edu/staff/hlm/2mass/overv/overv.html

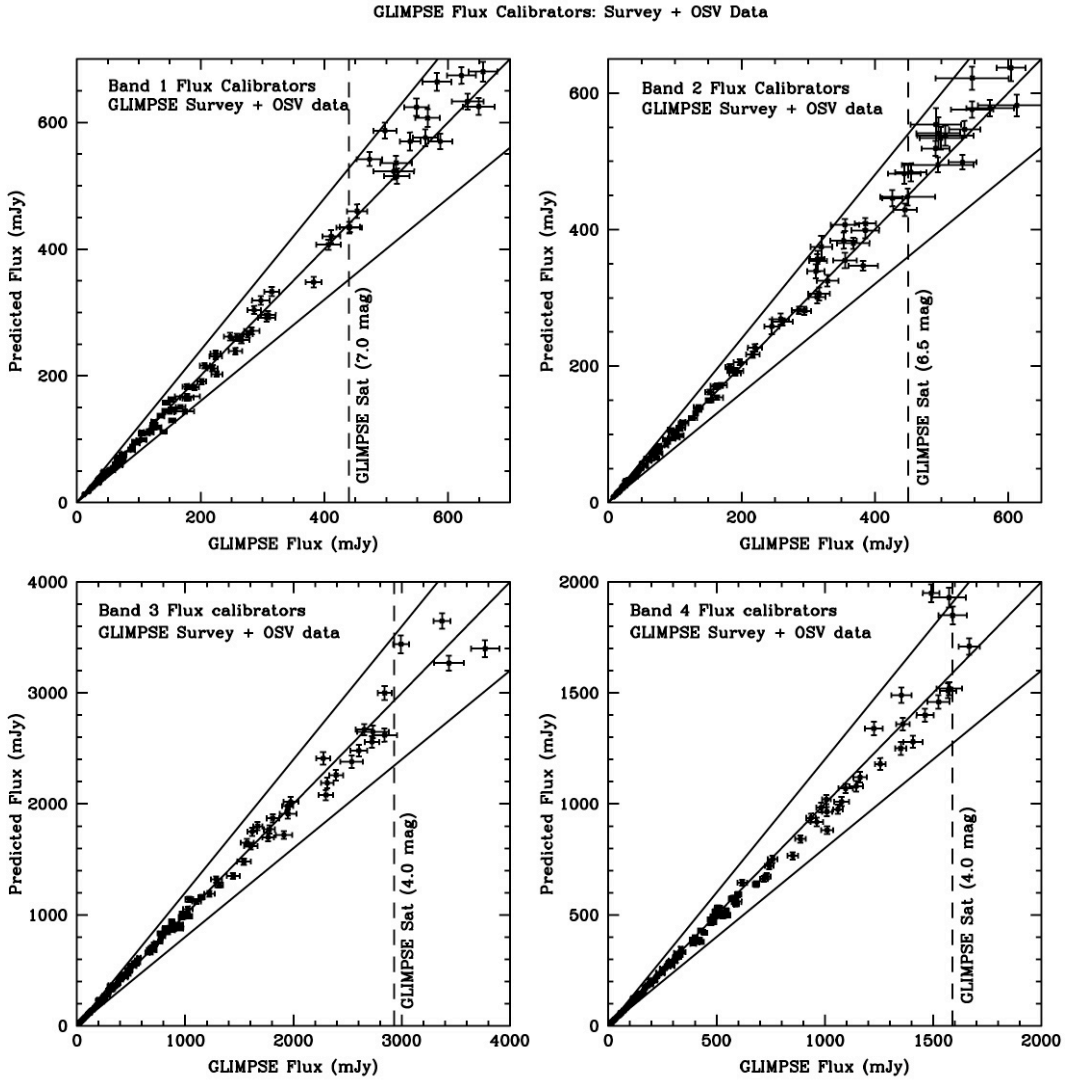

Figure 3. Comparison of the GLIMPSE extracted flux densities versus the predicted values for our network of flux calibrator sources. The wedge shaped boundaries indicate the flux density limits required for a photometric accuracy ≤0.2mag at each of the IRAC bands. The saturation limits are the dashed vertical lines. The extracted and predicted flux densities are well within the 0.2mag limit except for one source near the saturation limit in Band 4.

The systematic offsets do not have a measurable pattern when sampled at 10 degree intervals. However, samples taken over 12 arcmin intervals in the longitude range 306^0 to 310^0 have slightly larger random position differences in overlap regions of IRAC campaign boundaries, but even in these regions ~90% of the sources differ by ≤200 mas from 2MASS postitions and the remaining 10% do not exceed ~250 mas.

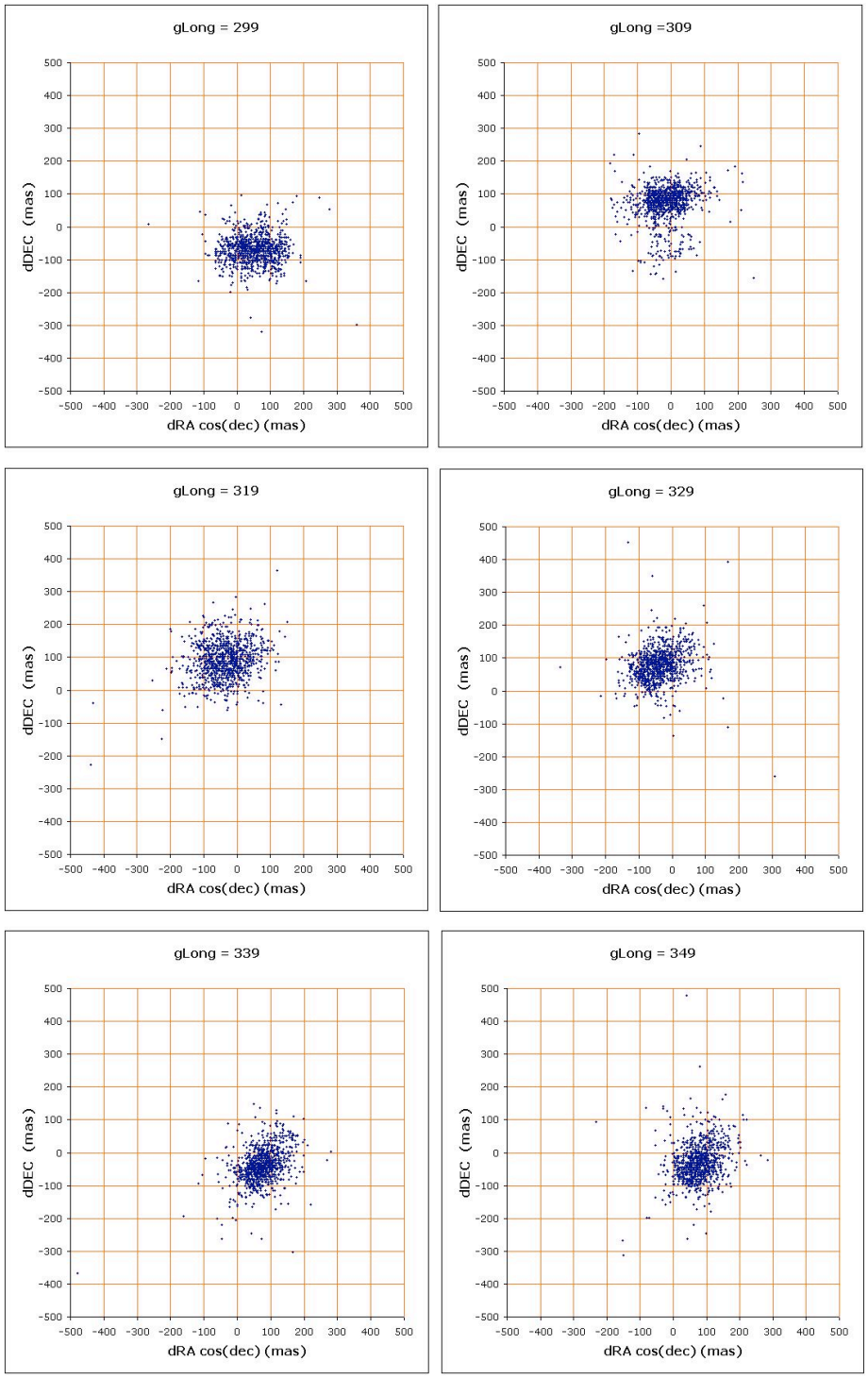

Figure 4. Spot diagrams showing the difference between GLIMPSE and 2MASS positions at 10^0 intervals in the southern Galactic plane. Here one sees both a systematic shift of ~100 mas and a random component of ~100 mas. Similar results are also seen in the northern plane.

To give a quantitative assessment of the offset in position between 2MASS and GLIMPSE we have chosen a sample of 10,000 sources (5000 each in the northern and southern plane) that are relatively uniformly distributed over the entire GLIMPSE survey area and that are detected in all three 2MASS bands and all four IRAC bands. These sources span a wide range of brightness, but of course do not represent the faintest sources in either catalog nor are bright sources near saturation in either catalog included. The cumulative fraction of all sources with position differences between GLIMPSE and 2MASS less than a given angular distance is plotted in Figure 5 for the northern and southern segments of the Galactic plane separately. 95% of all sources in the selected sample have position differences between 2MASS and GLIMPSE less than 200 mas; 99.9985% lie within 0.5"; 99.9995% within 0.75"; and, 99.9999% within 1.0".

We emphasize that Figure 5 only represents position differences between 2MASS and GLIMPSE determined for sources detected in all seven bands of 2MASS and GLIMPSE; it does not represent absolute position errors, which depend on the absolute astrometry of the 2MASS catalog.

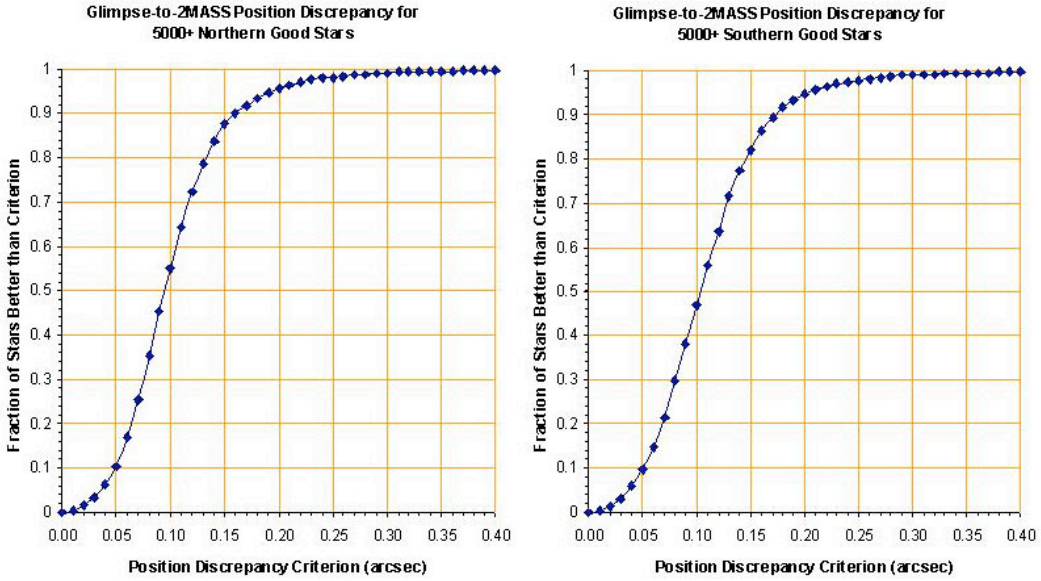

Figure 5. The cumulative fraction of stars detected in all 2MASS and all GLIMPSE bands with position differences less than the angular separation shown on the horizontal axis. A plot is shown separately for the northern and southern segments of the Galactic plane; 10,000 "good" stars (detected in all 2MASS and GLIMPSE bands) distributed relatively uniformly over the GLIMPSE survey area (5000 each in the northern and southern plane) are plotted.

VIII. Detection, Saturation, Confusion, and Background Limits

The GLIMPSE Catalog and Archive are constrained by: the detection limits, saturation (nonlinearity) limits, confusion limits, and, in some cases, diffuse background limits. Confusion and background limits depend on relative source brightness and other parameters, such as spatial variation of the background, in complex ways that defy specification by a single limiting parameter. In this section, we define how the GLIMPSE pipeline deals with these issues. In the bands where a source meets the selection criteria,

sources never dip below 5σ detections, although it is possible that the other bands can have 3≤S/N<5. No sources appear with S/N<3 in any IRAC band.

Table 2: GLIMPSE Dynamic Range

Type of Limit	Band 1	Band 2	Band 3	Band 4
3σ Detection Limit (mag)	15.5	15.0	13.0	13.0
Saturation Limit (mag)	7.0	6.5	4.0	4.0

Saturation Limits

GLIMPSE estimates of the saturation limits of each IRAC band were determined by a two-step process. First, simulated sources using the GLIMPSE derived point spread functions (PSFs) for each band were randomly populated in a simulated IRAC frame. The brightness of the sources was evaluated by checking if the brightest pixel for each source had exceeded the non-linearity limit (90% of full well). The magnitude limit was determined when simulated sources of a specific magnitude consistently showed the peak pixel exceeding the non-linearity limit. Second, we used our list of 277 flux calibrators to confirm and refine our estimates. Using the plots shown in Fig. 3, which show very good agreement between our extracted flux densities and Martin Cohen's predicted values, we were able to confirm and fine-tune the saturation limits to our observed data.

Confusion

Confusion depends in a practical sense on the local density of sources, the brightness contrast between the nearest source(s), the required photometric accuracy, and the brightness and spatial variation of the diffuse background emission. See the definition and extensive discussion of confusion with a list of relevant references on the SSC web page[7]. In Figure 6, we have attempted to quantify the dependence of confusion on the local stellar density and the average absolute difference between the true and extracted magnitude for a range of magnitude cut-offs. Ten simulated images were produced each with 2600-2700 stars of known magnitude randomly distributed between 7th and 15th mag. No sources were allowed to be closer than 2.5 pixels ~ 3 arcsecs (about two times the full-width at half maximum of the point spread function) to avoid source matching problems within and across IRAC bands. This corresponds to a source density of 400 sources/square arcmin. Fluctuating background emission was not included in the images because the main purpose here was to establish confusion limits (i.e. limits due to source crowding) independent of background limitations.

The average local source density was determined by expanding a box around each star until it enclosed at least five additional stars; this was then scaled to the number of stars per square arcmin. At any given density, the points in Fig. 6 represent the average of several hundred stars at each magnitude limit. The vertical axis in Figure 6 is the average absolute difference between the true flux density and the extracted flux density.
This is not the same as the photometric error of a given star, but rather indicates the decrease of photometric accuracy of the GLIMPSE point source extraction with increasing source density and decreasing brightness.

Band 1, with the highest density of all the IRAC bands, provides the most stringent test of confusion. The confusion limit is never reached for bands 3 and 4 in the GLIMPSE

[7] http://ssc.spitzer.caltech.edu/documents/compendium/resolution/confusion.html

survey. Figure 6 demonstrates that in Band 1, even at 14th mag., GLIMPSE flux densities depart from the true flux densities by <0.2 mag only for source densities >200 sources/arcmin^2. Densities of 200 sources/arcmin^2 are found in only a few of the most compact clusters. However, as source density increases, the percent of recovered sources decreases and the rate of decrease depends on the brightness limit. This is clearly illustrated in Figure 7 where we plot "completeness" (i.e. the fraction of true sources

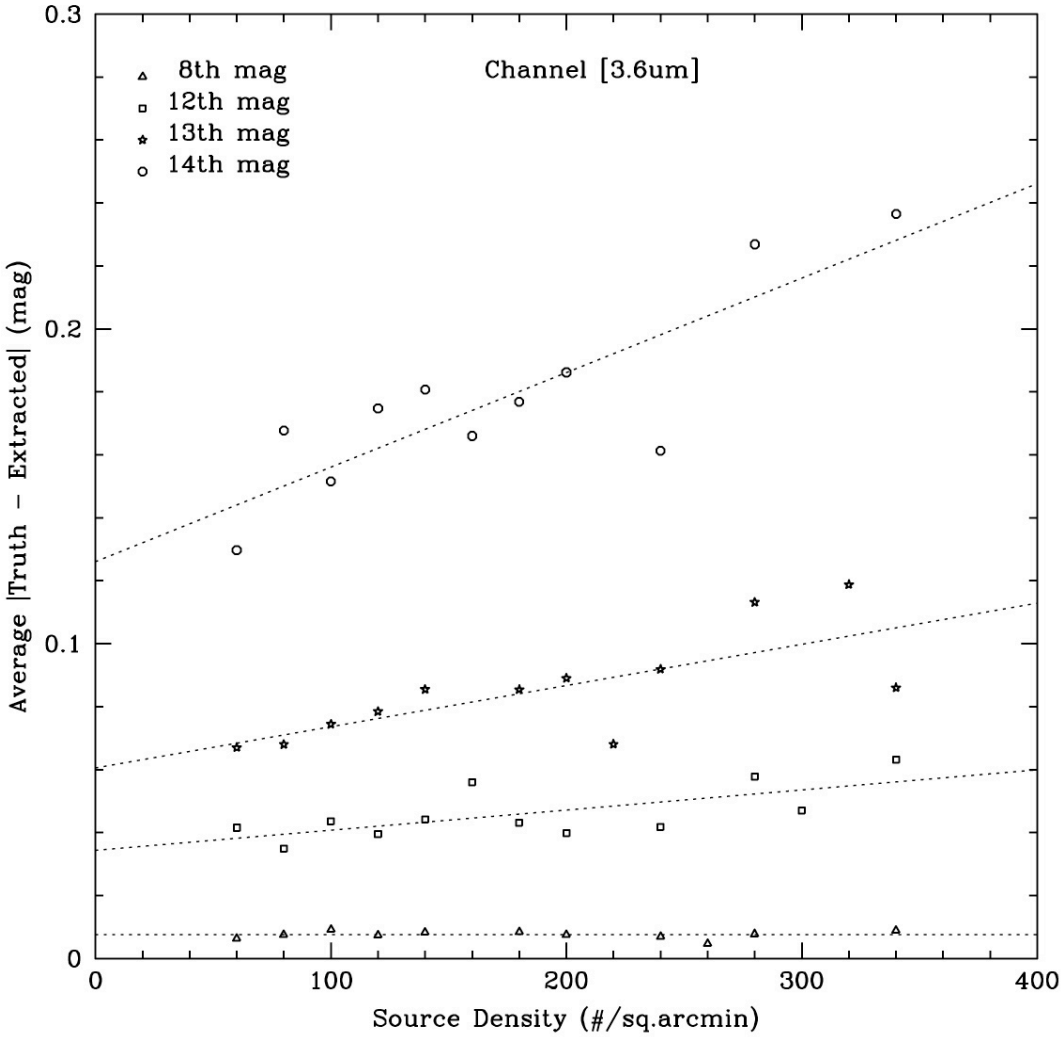

Figure 6. The average absolute difference between the true and extracted magnitudes of sources versus source density for a range of source brightness from 8th to 14th mag for Band 1. The curves do not go through the origin because the absolute difference always adds positively. These results are based on 10 simulated frames with a range of stellar brightness from 7th to 15th mag. Each frame contained 2600 to 2700 sources. Further description the simulations are in the text. The average extracted flux densities depart from the true flux densities with increasing source density as a function of source brightness. Only at 14th mag and fainter and at densities ≥200 arcmin^{-2} do average departures from the true magnitudes >0.2 mag begin to occur. The large dispersion at 14th mag is due to the faintness of the sources. At 13th mag and brighter, the average difference between the extracted and true magnitudes are well below 0.2 mag even at densities >300 stars arcmin^{-2}.

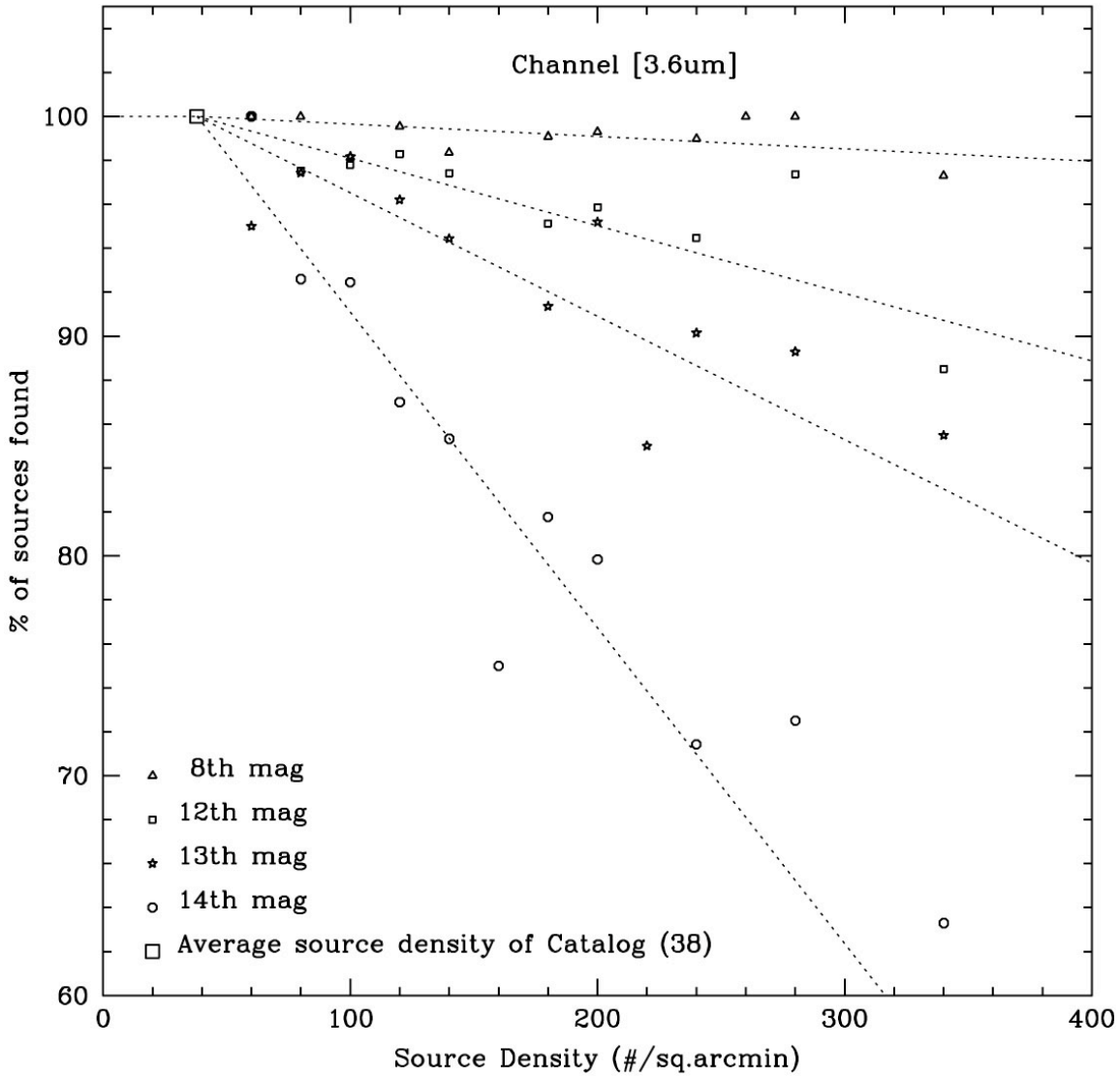

Figure 7. Completeness versus source density. The calculations shown here were obtained using the same simulations used in Figure 6. The average density of the Catalog (averaged over the entire survey) in IRAC Band 1 is 38 sources per square arcmin, indicated by the square.

extracted) as a function of both source density and brightness limit. Sources of 8th magnitude and brighter were greater than 98% complete out to densities of 340 arcmin^{-2}, whereas sources of 14th magnitude and brighter are only about 78% complete at densities of 200 arcmin^{-2}. 200 sources arcmin^{-2} is equivalent to an average separation between sources of ~4.2" or ~3.5 pixels. *We caution that the "completeness" shown in Fig. 7 is not the completeness of the GLIMPSE survey.* It is the completeness of a simulated field with known stellar content (truth table) as a function of stellar density and brightness in the absence of other effects that occur in the actual survey.

The analyses presented in Figs. 6 & 7 depend on simulated images, exclude sources closer than 3", and use the nearest 5 sources to estimate local density. The

Archive includes sources that are fainter than in the Catalog and closer than 3". We examine, in the following, the effects of nearest neighbors on photometry and the fraction of sources eliminated from the Archive by excluding sources with nearest neighbors closer than a given angular cut-off. In Figure 8, we plot the fraction of sources in the Archive with neighbors closer than a given angular distance against angular separation based on GLIMPSE sources within one square degree centered at galactic longitude 12.5^0. Eliminating all sources with neighbors closer than 2.5" would exclude about 10% of all sources in the GLIMPSE Archive according to Fig. 8.

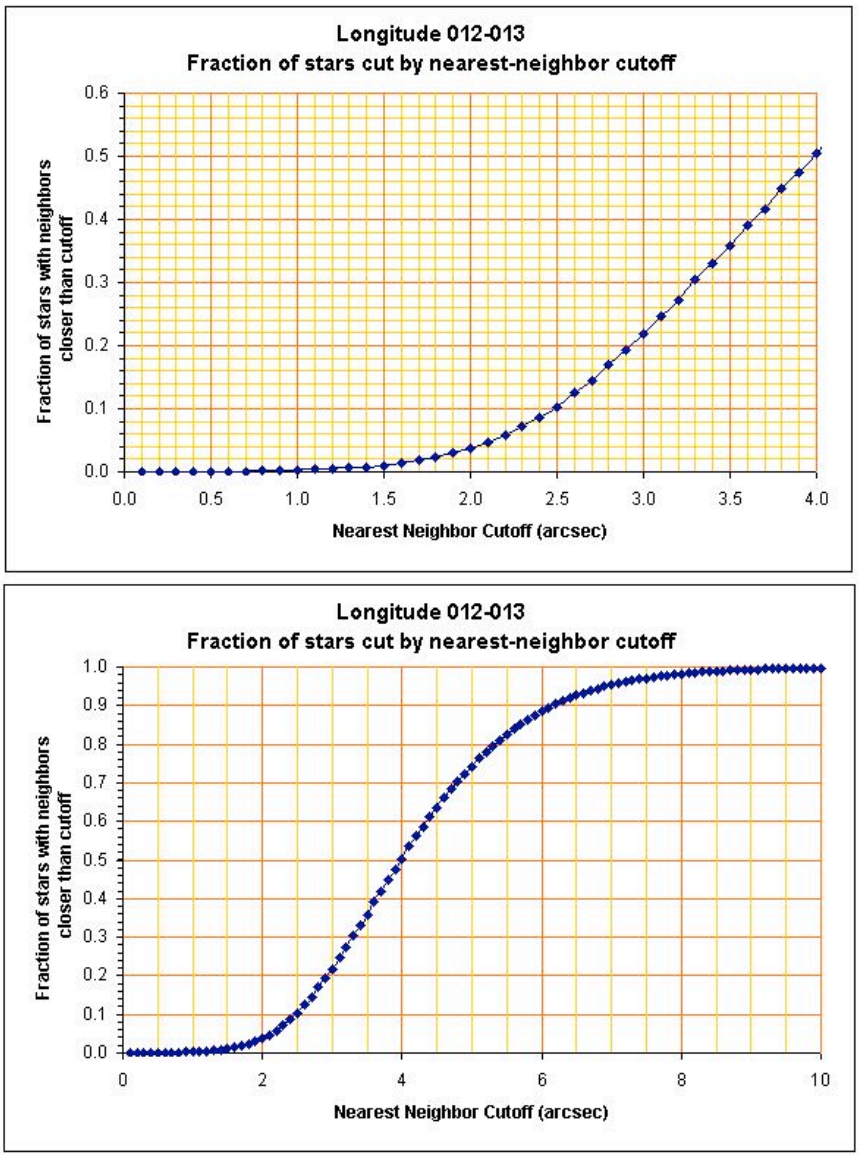

Figure 8. The cumulative fraction of sources that have nearest neighbors closer than a given angular distance versus angular distance. This figure is composed of sources in a square degree of the GLIMPSE survey centered at Galactic longitude 12.5^0. The upper panel is a zoomed-in version of the figure in the lower panel.

Figure 9 shows the distribution of angular separations of the three closest neighbors and the cumulative number of brightest sources within a given separation out to a radius of 36” (left panels) for sources in one square degree centered at longitudes 12^0 (upper panels) and 64^0 (lower panels). The right panels show the number of sources versus the distribution of brightness of the three nearest neighbors and the brightest source within a radius of 36”. Figure 9 demonstrates that the density of sources decreases at high galactic longitudes (no surprise), the brightness distributions of the three nearest neighbors are the same at a given longitude, and the peak of the brightness distributions are fainter with increasing longitude.

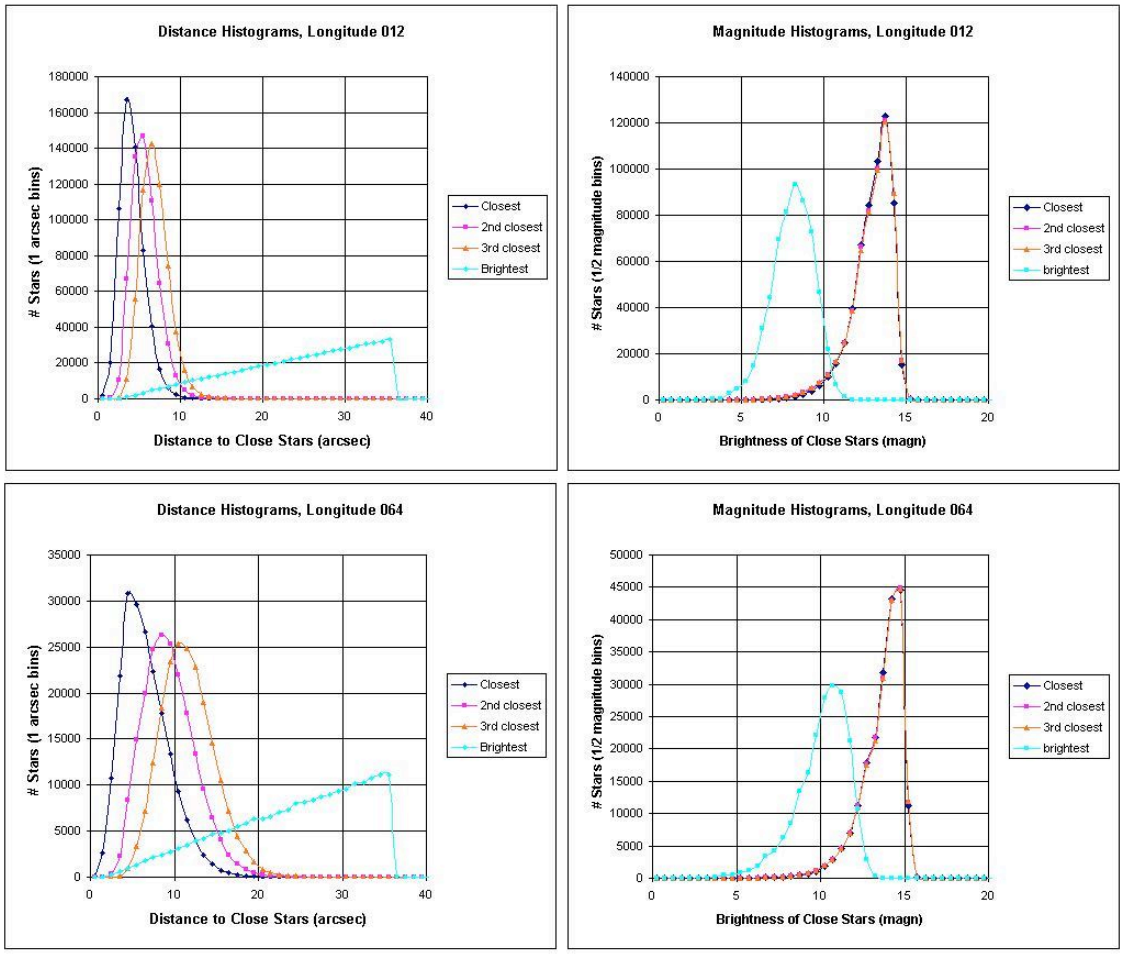

Figure 9. *Upper Panels*: Sources in an area of one square degree centered at longitude 12^0. *Left Panel;* The distribution of angular separations of the three closest neighbors and the cumulative number of brightest sources closer than a given angular separation. *Right Panel;* The brightness distributions of the three closest neighbors and the brightest source within a radius of 36”. *Lower Panels:* Sources in an area of one square degree centered at longitude 64^0. *Left panel*; same as that in the upper panel. *Right panel*; same as that in the upper panel.

Figure 10 illustrates how small angular separations between sources impacts stellar colors. The main effect here is that at separations less than about two pixels (~2.4 arcsecs) the phenomenon of "flux stealing" (i.e. assigning the fluxes of two close stars differently in two or more IRAC bands) becomes apparent. Stars located near longitude 12^0 were used to produce Fig. 10. In Fig. 10, the effect of flux stealing shows up as a spray of points running from the upper left to lower right in the color-color plots. The spray of points running toward the upper right is caused by interstellar reddening and is real. The magnitude range for each panel is labeled above each plot. The range was chosen such that a large enough number of stars were included for good statistics, but not so many that the separation at which flux stealing begins to be apparent is obscurred by too many points. Figure 10 shows that for separations less than about 2.4", flux stealing clearly becomes apparent.

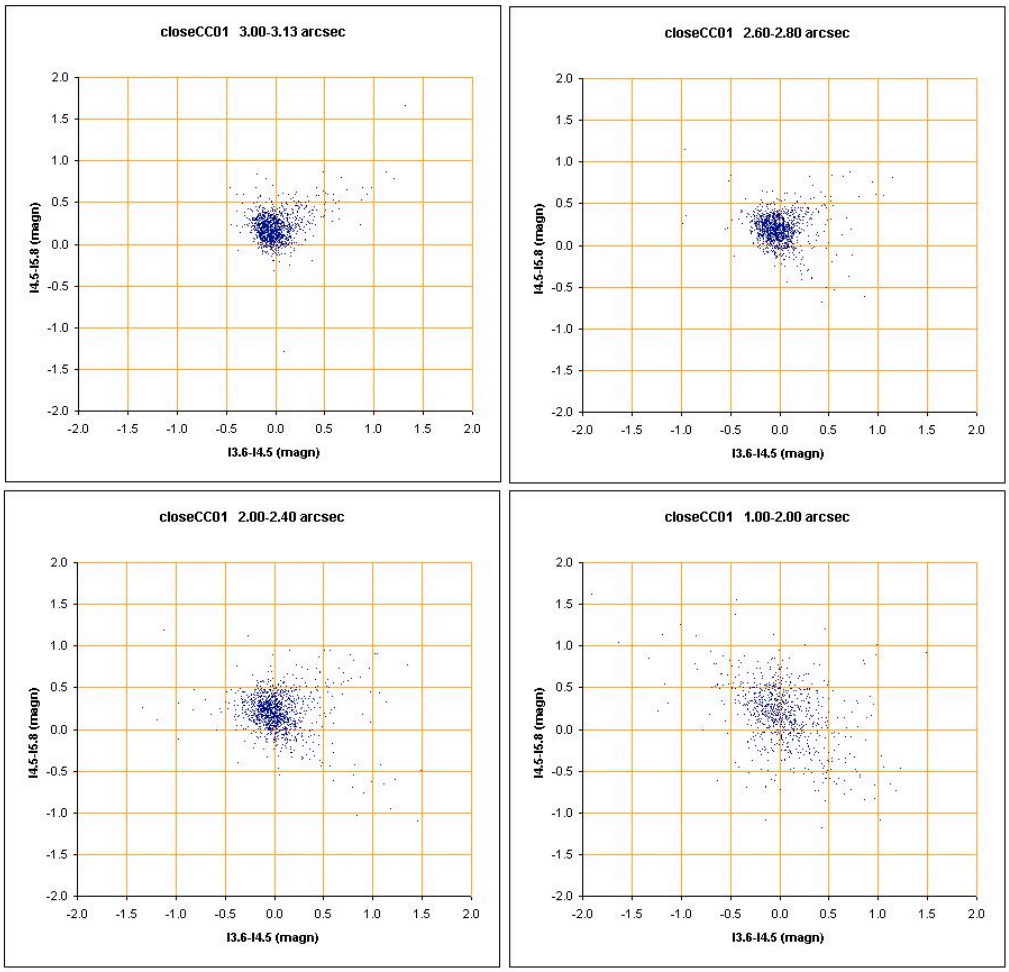

Figure 10. The 4.5-5.8 μm vs 3.6-4.5 μm color-color diagram for closest source separations 3.00"-3.13'' (upper left), 2.60"-2.80" (upper right), 2.00"-2.40" (lower left), and 1.00"-2.00" (lower right). This illustrates the impact on stellar colors of "flux stealing" or mis-assignment of the fluxes of two close stars in different IRAC bands. The stars in these plots include the whole range of stellar brightness shown in Fig. 9 at $\ell \sim 12^0$. At separations less than ~2.4", flux stealing becomes significant. Colors become unreliable at separations <2".

Fig. 6 and Fig. 10 seem to imply rather different limits on the closest neighbor. The reason for this is because the aims and techniques involved in forming the figures are different. Figure 6 used simulated images, determined average local density using the five closest sources, excluded sources with neighbors closer than 3", and did not include fluctuating background emission. Its main goal was to determine the maximum density (in the absence of other effects) at which the sources can be extracted with photometric accuracy ≤0.2 mag. Fig. 10, on the otherhand, was produced from actual GLIMPSE images and investigated the impact of "flux stealing" as a function of the closest neighbor. Figure 6 would give a more conservative estimate of the closest neighbor because it eliminated sources with neighbors closer than 3" and used a minimum of 5 sources to estimate the local density, whereas the analysis in Fig. 10 applied no minimum separation and was not concerned with the local density of sources.

In summary, our analyses indicates that all sources with a nearest neighbor closer than ~2.5" (two pixels; equivalent to 575 sources arcmin^{-2}) cannot be reliably extracted and bandmerged and should be considered as a single star. At 14th mag in Bands 1 & 2, we found that stellar brightnesses begin to have errors greater than 0.2 mag at source densities of ~200 stars arcmin^{-2} (mean separation ~4.2 arcsecs); at 13th mag and brighter photometric errors are substantially <0.2mag even at densities of 400 stars arcmin^{-2} (mean separation of 3").

Diffuse Background Emission

Source detection in elevated, complex background regions is problematic. To insure a high degree of reliability, the GLIMPSE pipeline employs several techniques to improve reliable source detection while minimizing false detections. The GLIMPSE pipeline smoothes the input image to produce an approximate background image. From this background image, a shifting 5x5 pixel box is used to determine the local background level. Since this is a local region and smoothed, we use the brightest value in the 5x5 pixel background box to set our initial 3σ detection limit. To further inhibit false detections on ridges, undulating backgrounds and steep inclines, the initial detection limit is scaled by a factor derived from the RMS fluctuations of the 25 pixels in the background box. When the RMS fluctuations of the background pixels in the box are small, then the background is flat and uncomplicated, and the scaling factor is 1.0. When the RMS is large, this means the range of values in the background is large, implying either a steep inclined background, or some small-scale complex background structure. The scaling factor is then greater than 1.0 and means detection will require a S/N>3.0. This mitigates much of the false source detection problems in complex background areas. However it may result in some missed sources where the source is located at the base of a steep background region. Examination of the images in bright complex background regions may show sources that are not in our Catalog because we have optimized source reliability over source completeness. See the GLIMPSE Pipeline Processing document for more details.

IX. Instrumental Artifacts and Cosmic Rays

The IRAC images contain several artifacts than can potentially impact the quality of the GLIMPSE data. Most of the instrumental artifacts discussed here are illustrated in

the Spitzer Observer's Manual[8] (SOM). The most obvious artifacts seen in the GLIMPSE data are muxbleed (bands 1 & 2), stray light patterns from bright sources outside the field (all bands), column pulldown (bands 1 & 2), banding (bands 3 & 4), cosmic rays (all bands); and detector saturation (all bands). We have searched for latent images from saturated sources and not found them in the GLIMPSE images, likely due to the short exposures and high backgrounds of the GLIMPSE data. The multiplexer bleed (muxbleed) effect is a series of bright pixels along the horizontal direction of a bright source in Bands 1 and 2. Column pulldown is a reduction in intensity of the columns in which bright sources are found in Bands 1 and 2. Banding refers to streaks that appear in the rows and columns radiating away from bright sources in Bands 3 and 4. These artifacts are described in detail in the *SOM* and the IRAC Data Handbook[9]. The GLIMPSE Pipeline Processing Document describes corrections in detail but a brief summary is outlined here.

Detector nonlinearity and saturation is dealt with in our photometry processing. We use information from the SOM and our comparisons to photometric standards (Figure 3) to determine the flux limits of our catalog. We mask saturated stars early in our processing pipeline using an algorithm that finds clusters of bright pixels.

The GLIMPSE pipeline corrects for column pulldown using an algorithm written by Lexi Moustakas of the Great Observatories Origins Deep Survey (GOODS) team, and modified to handle the highly variable backgrounds in the GLIMPSE fields. Our photometry algorithms are fine-tuned to deal with complex backgrounds, so the effects of column pulldown and banding on point source reliability are minimized. We corrected for banding using an exponential function. The SSC pipeline partially corrects for muxbleed, but does not correct all instances of this effect. The leftover muxbleed probably contributes the largest number of false sources to our Catalog (<0.4%) and Archive (<2%). SSC has provided software that will correct and flag leftover muxbleed which we will implement in our final 2006 data release.

Stray light patterns affect the quality of our mosaics, but not our point source reliability. The stray light regions are not masked for photometry, but will be flagged in the final Catalog and Archive release. The stray light regions are masked in our mosaicked images. SSC has provided an automated stray light masking program that uses the 2MASS catalog to find bright sources outside the frame. We have improved this algorithm using the GLIMPSE Catalog, which finds most (~98%) of the stray light patterns in bands 1 & 2. The rest (about 2 on average on a 1.1 x 0.8 degree mosaic) are found and masked by visual inspection. In bands 3 & 4, many of the stray light patterns repeat in the same place so are not easily removed. In cases where artifacts overlap in the same positions on multiple observations, we do not mask so that gaps in survey coverage do not occur. The stray light affects ~1% of the pixels in bands 1 & 2, and only ~0.08% in bands 3 & 4.

Cosmic rays also affect the quality of our mosaics but not our point source reliability. There are typically only 2-10 cosmic ray hits per frame, due to our short exposures. These are removed using the MOPEX[10] mosaic package with dual-outlier

[8] http://ssc.spitzer.caltech.edu/documents/som/

[9] http://ssc.spitzer.caltech.edu/irac/dh/

[10] http://ssc.spitzer.caltech.edu/postbcd/

rejection. Cosmic rays missed by the dual-outlier rejection are masked during visual inspection of the 1.1^0 x 0.8^0 mosaics.

In the following figures we show examples of images before and after corrections for banding, column pull-down, cosmic rays, and stray light.

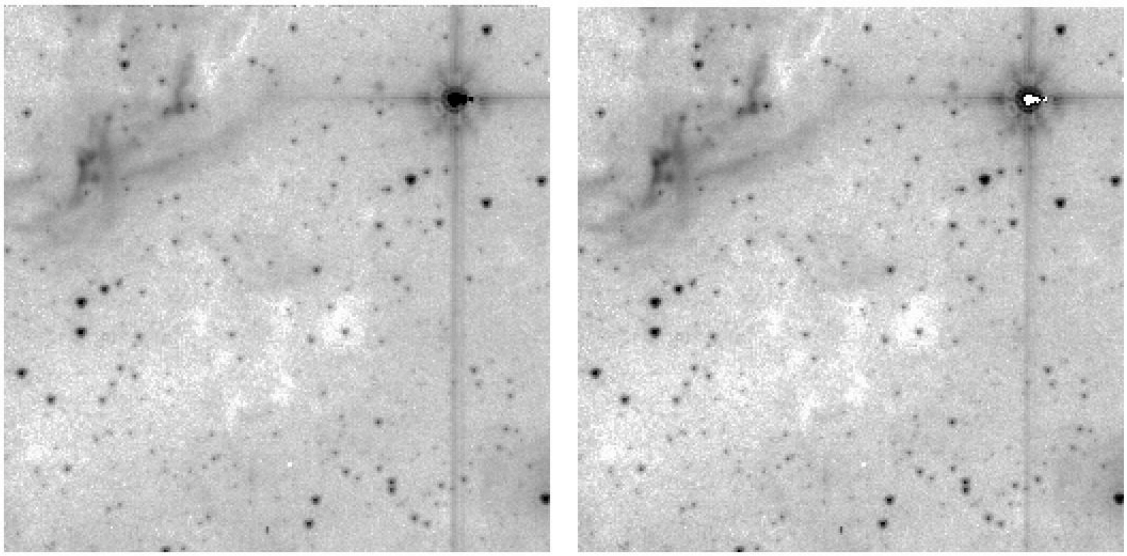

Figure 11 Example of banding due to a very bright star in IRAC Band 3 before correction (left panel) and after correction (right panel). For very bright stars, banding is obviously not completely removed.

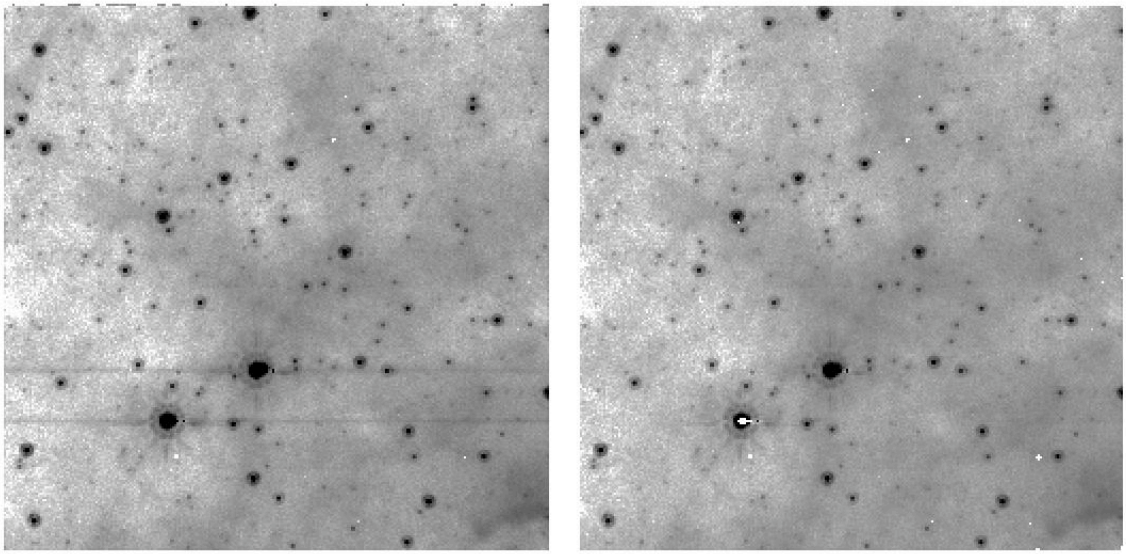

Figure 12 Example of banding in IRAC Band 4 of two intermediately bright stars before correction (left panel) and after correction (right panel). Banding correction in band 4 is better than for band 3.

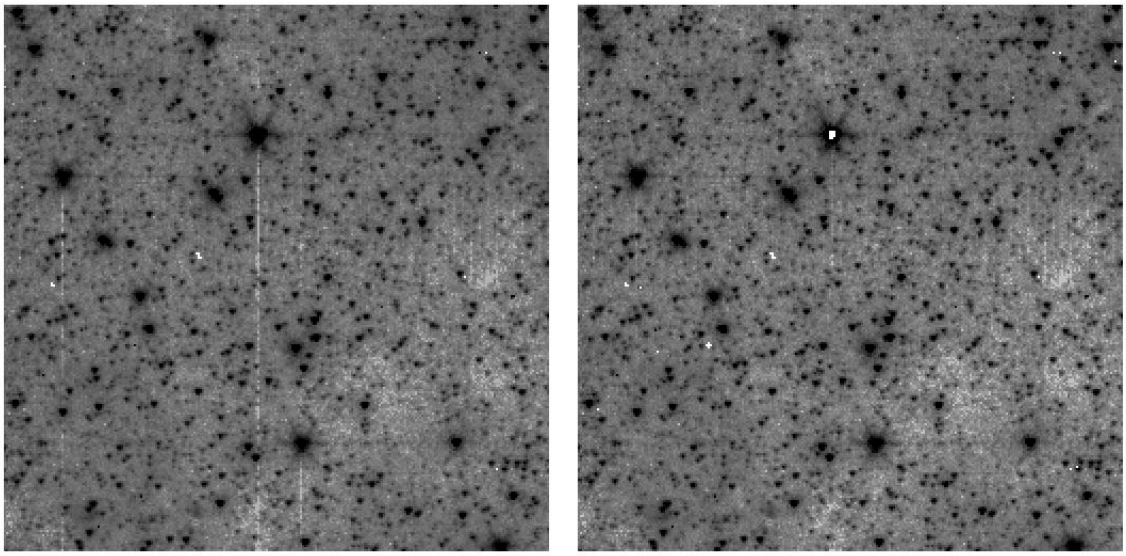

Figure 13 Example of column-pull down in IRAC Band 1 before correction (left panel) and after correction (right panel).

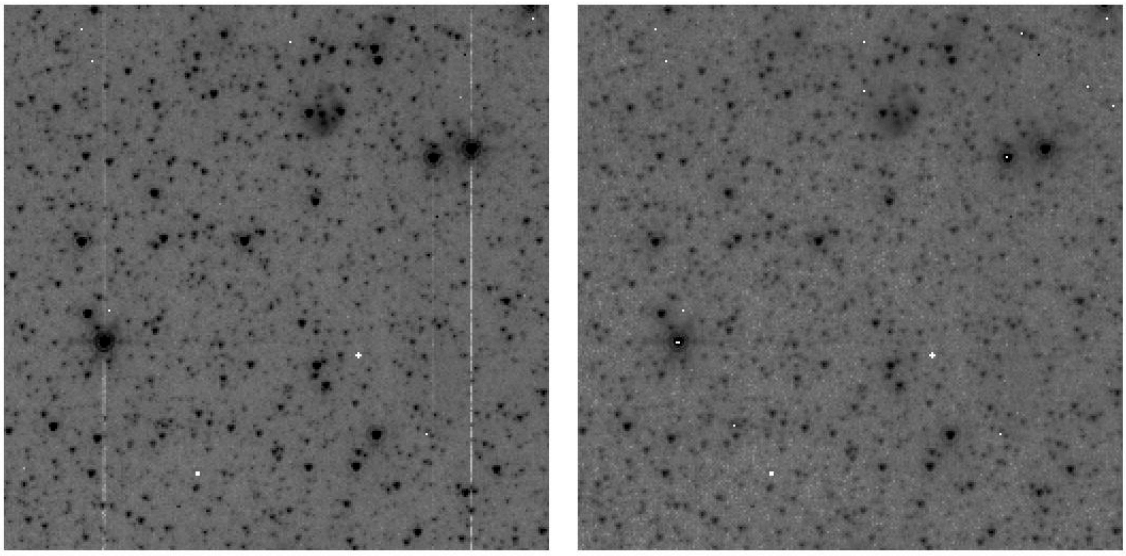

Figure 14 Example of column-pull down in IRAC Band 2 before correction (left panel) and after correction (right panel).

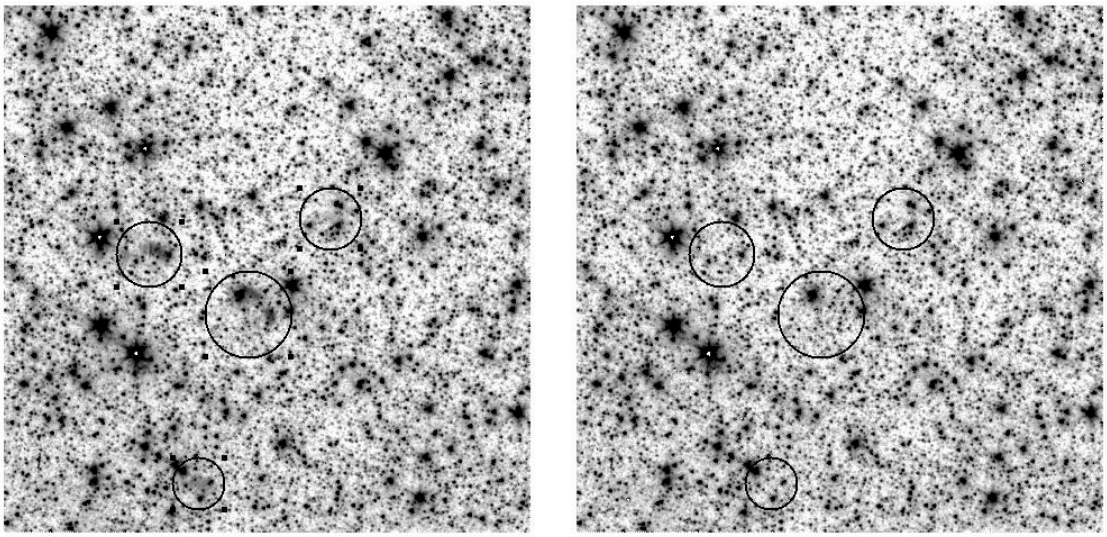

Figure 15 Left: Example of stray light in the circled regions in an IRAC Band 1 mosaicked image. Right: The same mosaicked field where the stray light patterns have been masked out in one of the frames.

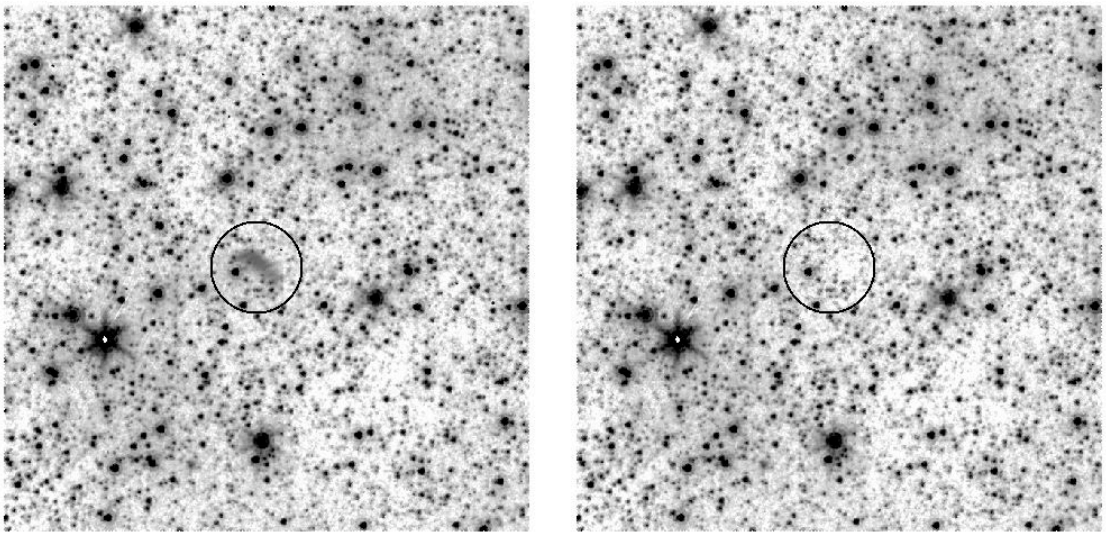

Figure 16 Left: Example of stray light shown in the circled region in an IRAC Band 2 mosaicked image. Right: The mosaicked image where the stray light has been masked out of one of the frames.

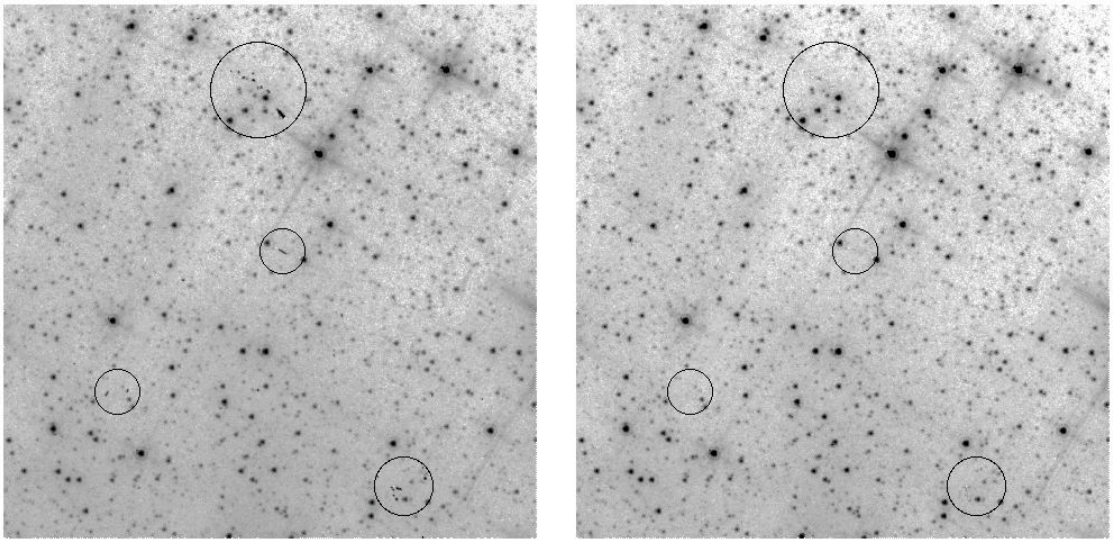

Figure 17 Example of cosmic ray hits (within circled regions) in an IRAC Band 3 mosaicked image before and after masking (right panel).

X. Summary

In this document we have described the observing strategy of the GLIMPSE survey; the criteria for selecting point sources for the GLIMPSE Catalog and Archive; the reliability and completeness of the Point Source Catalog; photometric and astrometric accuracies of the Point Source Catalog and Archive; detection, brightness, confusion, and background limits; and corrections for instrumental artifacts. The main effects that impact the quality of the GLIMPSE data have been addressed in this document. A brief summary of the major properties of the GLIMPSE program are given below.

Summary: GLIMPSE Properties

Areal Coverage:	Longitude: 10^0 to 65^0 and 350^0 to 295^0 Latitude: $\pm 1^0$			
Reliability:	≥99.5% (Catalog)			
Completeness[11]:	≥65% (Catalog)			
Catalog:	30,252,689 sources (single frame photometry)			
Archive:	47,722,247 sources (single frame photometry)			
Positional Accuracy:	95% <200 mas relative to 2MASS			
Photometric Accuracy:	0.2 mag (see Table 1 and explanation in the text)			
Confusion Limits[12] (no. arcmin^{-2}):	~240 (≤14th mag)	>340 (≤13th mag)		
	Band 1	Band 2	Band 3	Band 4
Dynamic Range (mag)[13] :	15.5-7.0	15.0-6.5	13.0-4.0	13.0-4.0

[11] Most of the incompleteness occurs near the sensitivity limits which are approximately: 13.9, 13.6, 12.1, and 11.4 mags for Bands 1-4, respectively, for the Catalog and approximately 14.2, 13.9, 12.1, and 11.4 mags, respectively, for bands 1-4 for the Archive.

[12] See Figure 6. At densities ≤240 sources per square arcmin the average departures of the extracted magnitudes from the true magnitudes are less than 0.2mag for sources 14th mag and brighter in Band 1. For sources of 13th mag and brighter, the average of extracted versus true magnitudes do not exceed 0.2 mag differences for densities well in excess of 340 per square arcmin in Band 1. Since Band 1 has the highest density of sources, it is expected to suffer the most severe confusion. A few very dense clusters are confusion limited in Bands 1 & 2, but Bands 3 and 4 are never confusion limited in the GLIMPSE survey.

[13] 3σ limit at the faint end and saturation limit at the bright end.

X. References

Cohen, M. 1993, AJ, 105, 1860

Cohen, M. 1994, AJ, 107, 582

Cohen, M. 2006, in preparation

Cutri, R. M. et al. 2003, Explanatory Supplement to the 2MASS All Sky Data Release http://www.ipac.caltech.edu/2mass/releases/allsky/doc/explsup.html

Price, S. D. Egan, M. P., Carey, S. J., Mizuno, D. R., & Kuchar, A. 2001, AJ, 121, 2819

Stetson, P. B. 1987, PASP, 99, 191

Wainscoat, R. J., Cohen, M., Volk, K., Walker, H. J., & Schwartz, D. E. 1992, ApJS, 83, 111

XI. Glossary of Acronyms

AOR----------Astronomical Observing Request
Archive-------GLIMPSE Point Source Archive
BCD----------Basic Calibrated Data
Catalog-------GLIMPSE Point Source Catalog
FWHM-------Full-width at half maximum
GLIMPSE—Galactic Legacy Infrared Mid-Plane Survey Extraordinaire
IRAC---------InfraRed Array Camera
IRAC Bands-1, 2, 3, and 4 have central wavelengths of 3.6, 4.5, 5.8, and 8.0 μm
ISDS----------IRAC Science Data Simulator
OSV----------Observation Strategy Validation
PSF----------Point Spread Function
SOM---------Spitzer Observer's Manual
S/N----------Signal-to-noise